https://doi.org/10.22226/2410-3535-2021-4-561-565 PACS: 72.80.Tm

Check for updates

Molecular dynamics investigation of atomic mixing and mechanical properties of Al/Ti interface

P. V. Polyakova[†,1], S. A. Shcherbinin[2], J. A. Baimova[3,4]

[†]polina.polyakowa@yandex.ru

[1]Ufa State Petroleum Technological University, Ufa, 450062, Russia
[2]Peter the Great St. Petersburg Polytechnic University, St. Petersburg, 195251, Russia
[3]Institute for Metals Superplasticity Problems, RAS, Ufa, 450001, Russia
[4]Bashkir State University, Ufa, 450076, Russia

With the urgent lightweight demand in the aerospace engineering and transportation industries, Al/Ti composite structures have attracted much interest due to their excellent performances compared with conventional materials. Computational simulations have contributed to the understanding of both fundamental and practical aspects of fabrication of such composites and studying of their properties. The present work reports the results of studies based on molecular dynamics simulations on the mechanical properties of an Al/Ti composite obtained by compression combined with shear strain. Tensile properties of a nanosized Ti/Al composite consisting of two single crystals obtained after different compression rates are analyzed. The loading scheme applied in the present work is a simplification of the scenario experimentally realized previously to obtain Al-matrix composites. It is confirmed that uniaxial compression combined with shear deformation is an effective way to obtain the composite structure since severe plastic deformation facilitates the diffusion process. The results indicated that a symmetrical atomic movement took place in the Ti/Al interface during deformation. However, Al atoms diffuse into the Ti block easier than Ti atoms into the Al block. Tensile tests showed that fracture took place in the Al part of the final composite sample, which means that the interlayer region where the mixing of Ti and Al atoms is observed is stronger than the pure Al part.

Keywords: composite, molecular dynamics, titanium, aluminum, mechanical properties.

1. Introduction

Recently, research attention has been directed towards the development of new materials such as composites which can have improved properties in comparison with traditional alloys and metals. The combination of strength and ductility of Ti/Al composites attracts great attention since such materials can be effectively applied in the automobile and aerospace industries [1, 2].

The process of fabrication of new composites is an important problem since the fabrication method considerably affects their physical and mechanical properties. Some very effective methods allow processing *in-situ* composites, where the intermetallic phases are obtained naturally during the fabrication process. These composites can demonstrate very unusual physical and mechanical properties. As it was shown previously, severe plastic deformation is an effective method of composite fabrication, which allows obtaining Al/Cu, Al/Nb, and Al/Ti *in-situ* metal-matrix composites with improved hardness [3 – 9]. The formation of intermetallic phases during severe plastic deformation is facilitated due to faster diffusion [10]. However, commonly TiAl is obtained by the melting-casting route and, thus, intermetallic structure is fabricated by very different way and has lower ductility.

Unfortunately, detailed experimental studies of phase and structural transformations are expensive and difficult and often cannot be realized. Computer simulation can provide insight into the atomic mechanisms of deformation, giving a fundamental understanding of strategies for the fabrication of composites with improved properties. Molecular dynamics (MD) simulation has emerged as a suitable tool to investigate different kinds of phenomena in materials, such as plastic deformation and tensile properties [11–13], irradiation damages [14], composite fabrication [15 –17], alloying reaction [18,19], to name a few [20 – 24].

In the present work, MD simulation is utilized to analyze the role of applied strain on the mechanical performances of Al/Ti composites obtained by the combination of compressive and shear strain. The mixing of atoms near the interface between Al and Ti during deformation is analyzed.

2. Computational methods

To study the process of atomic mixing under deformation treatment near the interface of different metals, MD simulation of an Al/Ti sample containing an interfacial boundary is used. The cubic sample containing 50 072 atoms is a simulation box with dimensions of 10×10×10 nm^3.

The Ti (upper) and Al (bottom) layers are 5.0 nm thick. The interlayer distance between two crystals was set equal to an average of lattice parameters of two crystals, $(a_{Ti}+a_{Al})/2=3.5$ Å. The calculations are performed using NVT ensemble and periodic boundary conditions in all directions. The suitability of periodic boundary conditions is justified in accordance with the experimental technique considered as the example: several plates of different metals, combined like Al/Ti/Al. The parameters for both metals important to analyze the diffusion behavior under compression are presented in Table 1.

The simulations are carried out using the LAMMPS (Large-scale Atomic/Molecular Massively Parallel Simulator) free simulation package [25]. For temperature control, the Nose-Hoover thermostat is applied to preserve the room temperature. Verlet algorithm is used to integrate the Newtonian equations of motion with an integration time-step of 2 fs. Visualization of MD data and structure analysis have been carried out using Open Visualization Tool (OVITO) [26]. The common neighbor analysis (CNA) [27] and the dislocation analysis are used to analyze the evolution of atomic configurations and the dislocation motions in the sample.

An embedded atom method (EAM) interatomic potential for Ti and Al is used [28]. The potential is fitted to both experimental and *ab-initio* data of different crystal properties and structures in the Ti/Al system and gives a good description of fundamental properties, for example, defect energies, lattice properties, and thermal expansion [28 – 30]. The deformation behavior of Ti/Al using various potentials was tested under uniaxial tension in a wide range of temperatures. It was shown that this potential can be effectively used for the study of mechanical properties and deformation. This potential is suitable particularly for describing the deformation and fracture mechanisms of Ti/Al systems.

The simulation process consists of several steps. At first, the simulation box was equilibrated at 300 K. Then, to study the process of fabrication of Ti-Al composite and phase transformation in the system, strain along the *z*-axis, ε_{zz}, combined with shear strain in the *xy*-plane, ε_{xy}, is applied. Compression is combined with shear to reproduce the high-pressure torsion experimental techniques [3 – 6]. Strain rates are $\dot{\varepsilon}_{zz}=6.2\times10^{-8}$ ps^{-1} and $\dot{\varepsilon}_{xy}=6.2\times10^{-7}$ ps^{-1}.

In the last step, the tensile loading normal to the Al/Ti interface is applied ($\varepsilon_{zz}>0$ in this case) which allows analyzing the tensile behavior of the obtained composite. Simulations of tensile tests are conducted at 300 K, which is usual for experiments. The tensile strain imposed in this simulation is performed by deforming the simulation box. During the dynamic loading, the stress is attained by the averaged stress, and the strain is derived from the positions of the periodic boundaries along the *z*-axis.

3. Results and Discussion

3.1. Atomic mixing under compression

In Fig. 1, the stress-strain curve for the sample under compression is presented along with the snapshots of the structure at three strain stages. Simulated tensile tests were applied to the initial structure and to the system after carrying out three steps of compression deformation indicated by points I, II, and III in Fig. 1. In other words, the structures of the composite obtained after compression to points I, II, and III are considered as initial ones for tensile tests without an additional relaxation or changes. Thus, these structures in Fig. 1 are considerably compressed and non-equilibrium. The structures are visualized in accordance with common-neighbor analysis (CNA): green atoms belong to the FCC lattice, red atoms have an HPC environment, and gray atoms are those which have a different coordination number (undefined). During simulations, Al atoms leaving the calculation domain through the lower boundary entered the upper part formed by Ti atoms through the upper boundary of the simulation box. As a result, Al atoms were instantaneously transported to the upper boundary of the Ti plate and diffused towards that plate. Thus, there are two interfaces for atomic diffusion. Dislocation analysis showed that dislocations appeared on the Al/Ti interface right after initial relaxation which means that coherent interface is obtained with the mismatch.

Several pop-in events are observed on the stress-strain curves, which can be attributed to the release of strain energy accumulated during the deformation through defect activities. The shape of the curve up to point I ($\varepsilon_{zz}=0.076$) is almost linear, without significant stress fluctuations, on contrary to its shape between points I to II and II to III. Initial structure has two parts with clearly defined lattices (red for Ti

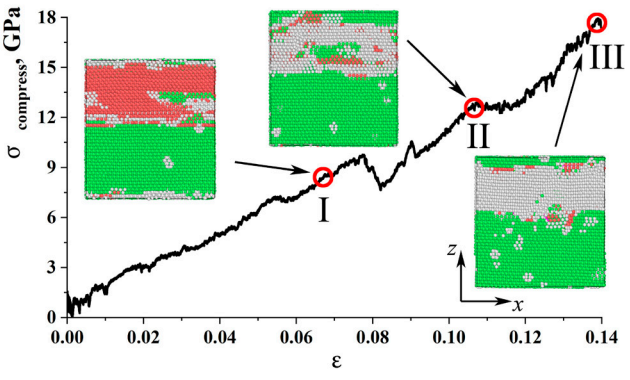

Fig. 1. (Color online) Stress-strain curves during uniaxial compression normal to the Al/Ti interface combined with shear in the interface plane. Snapshots of the structure in accordance with common-neighbor analysis (CNA): green atoms belong to FCC lattice, red atoms have an HPC environment, and gray atoms have a different coordination number (undefined).

Table 1. The parameters for Al and Ti, important to analyze the diffusion behavior under compression.

Metal	Lattice structure	Lattice parameters, Å	Atomic radius, pm	Atomic mass, g/mol	Melting temperature, °C
Al	FCC	$a=4.05$	143	26.98	660
Ti	HPC	$a=2.951$ $c=4.697$	147	47.867	1 668

and green for Al). Such an order is preserved until point I, as it can be seen from snapshots. During compression process, the titanium lattice was compressed so strongly that the program cannot determine the type of crystal lattice and Ti part of the crystal is shown in gray after point I. Moreover, part of the composite, where the mixture of Al and Ti atoms took place is also shown by gray, since OVITO cannot distinguish intermetallic phases.

In Fig. 2, concentration of Ti (upper part) and Al (lower part) near the Al/Ti interface at three strain values is presented. Only a part of the sample in the middle (40 Å thick) where atomic mixing took place is shown. The initial position of the interface is shown by a black dashed line. Even during the early simulation steps ($\varepsilon_{zz} < 0.04$), the interface boundary moves from Al part towards the Ti one by 3 Å. Red line shows the interface after breaking of the lattice symmetry for Ti, when continuous movement of the interface from Al to Ti is found. After $\varepsilon_{zz} = 0.14$, interface moved for 9 Å in comparison with the initial position.

In Fig. 3, molecular configurations (Al atoms are shown on the left and Ti atoms — on the right side) through Al/Ti interface for $0.0 < \varepsilon_{xy} < 0.14$ are presented. Ti block in the model is shifted to the right by about 100 Å for a clearance. During deformation treatment, considerable mixing of Al and Ti atoms took place through the interface. As was shown by the numerical analysis of average and maximum distances of an atomic displacement in comparison with the initial position of the boundary, the value of atomic displacement rapidly increases for $\varepsilon_{zz} = 0.04$. After that strain value, more Ti and Al atoms move towards each other, but the values of displacement (both average and maximal) remain almost constant. In common, average (maximal) displacement of Al and Ti atoms towards each other is equal, which means that diffusion is quite symmetric.

As it can be seen, Ti atoms move faster in the central part of the sample (Fig. 3 a, left side, pink and blue dots), while Al atoms move faster at the edges (Fig. 3 a, right side, green and purple dots). During compression up to the strain of $\varepsilon_{zz} = 0.04$, near the mixing interface, Ti atoms move more actively than aluminum atoms and pass into the Al part for about 14 Å; however, after $\varepsilon_{zz} = 0.04$, Ti atoms practically do not change their positions. As a result, at $\varepsilon_{zz} = 0.14$, the number of Al atoms diffusing into the Ti block is greater than the number of Ti atoms diffusing into the Al block. The interface between Al and Ti became blurred and chaotic after $\varepsilon_{zz} = 0.04$ forming a narrow diffusion zone, as shown in Fig. 3. Subsequently, more and more atoms participated in diffusion, and the thickness of diffusion zone increased with the simulation time (strain value). The symmetry of diffusion is related to material parameters of Al and Ti [31,32]: the differences in their melting points and atomic radii are insignificant (see Table 1).

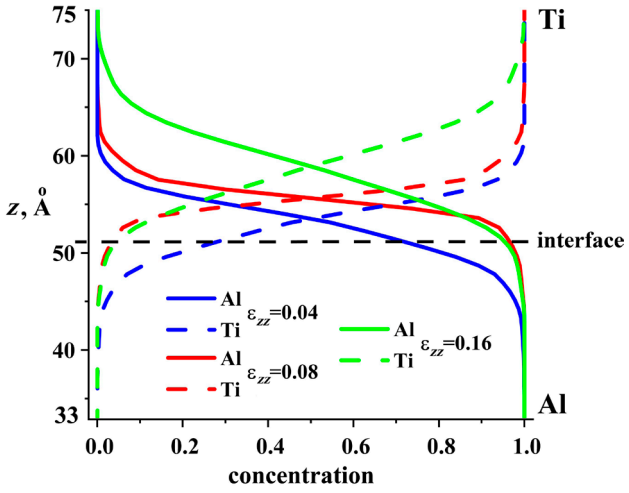

Fig. 2. (Color online) Concentration of Ti (upper part) and Al (lower part) near the Al/Ti interface at three strain values. Only part of the sample in the middle (40 Å thick) where atomic mixing took place is presented. The initial position of the interface is shown by black dashed line.

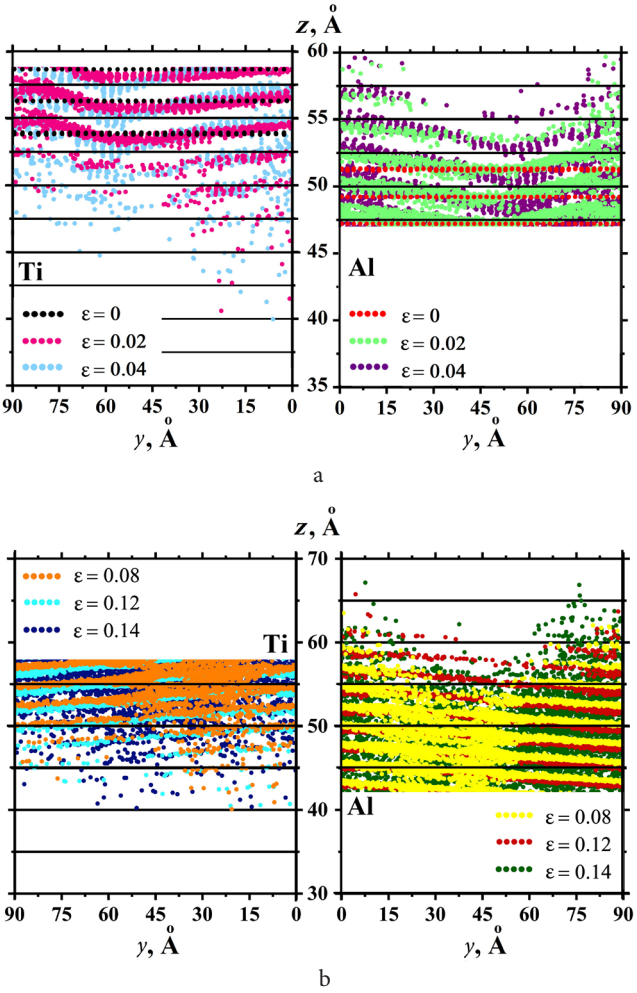

Fig. 3. (Color online) Molecular configurations of atoms (Al atoms are shown in the left and Ti atoms — in the right side) in the cross-section: for $0.0 < \varepsilon_{xy} < 0.04$ (a) and for $0.04 < \varepsilon_{xy} < 0.14$ (b). Ti block in the model is shifted to the right by about 100 Å for a clearance. Different colors correspond to different deformation stages. Only a part of the sample in the middle part (40 Å thick) where atomic mixing took place is presented.

3.2. Tensile behavior

To study mechanical properties of the obtained composite, uniaxial tension along the *z*-axis is applied after different levels of compression. In Fig. 4, stress-strain curves during tensile loading normal to the Al/Ti interface are presented for the tension of the initial sample (blue curve) and tension

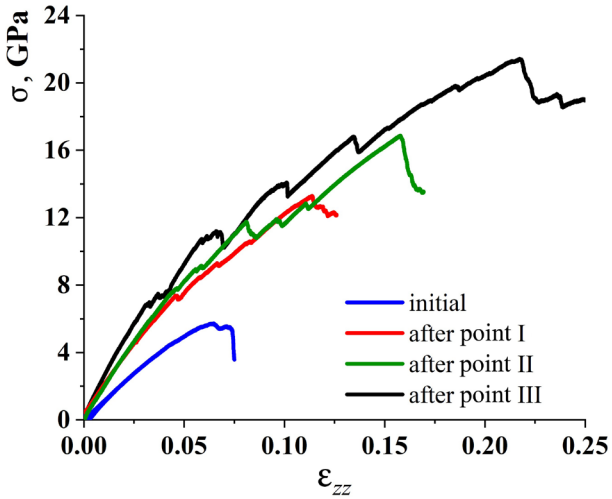

Fig. 4. (Color online) Stress-strain curves during tension normal to the interface region after different initial compression strain: after ε_{zz} = 0.068, ε_{zz} = 0.107 and ε_{zz} = 0.14.

after compression at stages I (red curve), II (green curve), and III (black curve). Several pop-in events are observed on the stress-strain curves, which can be attributed to the release of strain energy accumulated during the deformation through defect activities. All the critical strains and strengths are presented in Table 2.

During tension, the titanium lattice is restored, as a result of which stress spikes are observed on the curve, and the CNA analysis shows the appearance of an HCP lattice in the sample. Dislocation analysis showed that during tension dislocations can be found near the Al/Ti interface for any of obtained composites near the upper and lower boundaries. Some dislocations can also be observed in the Al part of the composite, however, after high strain level, dislocations almost disappear from the both parts of simulation box.

With an increase in the applied compressive (shear) stress, the strength of the composite is increased. It should be noted, that the curves after points II and III are very similar, which means that composite structure was obtained after point II. All the obtained composites with Al/Ti interface have much higher strength than the initial bimetallic sample.

Table 2. Tensile strain and strengths of tension normal to the interface region after different initial compression strain: after ε_{zz} = 0.068 (I), ε_{zz} = 0.107 (II) and ε_{zz} = 0.14 (III).

Structure state	Tensile strain	Tensile strength, GPa
initial	0.074	5.1
I	0.112	13.2
II	0.157	16.8
III	0.215	22

4. Conclusion

In the present paper, the process of formation of Al/Ti composite from two initially separated crystals by severe plastic deformation (compression combined with shear) is analyzed on an atomistic level by MD simulation. The proposed model is the simplification of scenario experimentally observed previously: in experiments [3 – 6], the samples are polycrystals, while in the present model a system consisting of two single crystals is considered to better understand the atomic mixing in the Al/Ti interface.

It is found that such a deformation treatment is an effective way to obtain the composite structure. Shear strain plays the most important role and considerably accelerates the atomic mixing. The analysis shows that Al atoms diffuse into Ti block easier than Ti atoms diffuse into Al block which is connected with the similarity of atomic radii and melting temperatures of Al and Ti. Tensile tests showed that fracture took place in the Al part of the final composite sample, which means that the interlayer region where the mixing of Ti and Al atoms observed is stronger than the pure Al part.

Acknowledgments. Work of JAB (methodology, analysis, paper writing) was supported by the State Assignment of IMSP RAS. Work of PVP (numerical calculations) was supported by the grant of Russian Science Foundation (No. 20-72-10112). SAS wish to acknowledge Peter the Great Saint-Petersburg Polytechnic University Supercomputer Center "Polytechnic" for computational resources.

References

1. Y. Du, G. Fan, T. Yu, N. Hansen, L. Geng, X. Huang. Mater. Sci. Eng. A. 572, 673 (2016). Crossref
2. M. Yamaguchi, H. Inui, K. Ito. Acta Mater. 48 (1), 307 (2000). Crossref
3. R. R. Mulyukov, G. F. Korznikova, K. S. Nazarov, R. K. Khisamov, S. N. Sergeev, R. U. Shayachmetov, G. R. Khalikova, E. A. Korznikova. Acta Mech. 232 (5), 1815 (2021). Crossref
4. G. F. Korznikova, E. A. Korznikova, K. S. Nazarov, R. U. Shayakhmetov, R. K. Khisamov, G. R. Khalikova, R. R. Mulyukov. Adv. Eng. Mater. 23 (1), 2000757 (2020). Crossref
5. G. R. Khalikova, G. F. Korznikova, K. S. Nazarov, R. U. Khisamov, S. N. Sergeev, R. U. Shayakhmetov, R. R. Mulyukov. Lett. Mater. 10 (4), 475 (2020). (in Russian) [Г. Р. Халикова, Г. Ф. Корзникова, К. С. Назаров, Р. Х. Хисамов, С. Н. Сергеев, Р. У. Шаяхметов, Р. Р. Мулюков. Письма о материалах. 10 (4), 475 (2020).] Crossref
6. V. N. Danilenko, S. N. Sergeev, J. A. Baimova, G. F. Korznikova, K. S. Nazarov, R. U. Khisamov, A. Glezer, R. R. Mulyukov. Mater. Lett. 236, 51 (2019). Crossref
7. A. Bartkowska, P. Bazarnik, Y. Huang, M. Lewandowska, T. G. Langdon. Mater. Sci. Eng. A. 799, 140114 (2021). Crossref
8. K. Ohishi, K. Edalati, H. S. Kim, K. Hono, Z. Horita. Acta Mater. 61 (9), 3482 (2013). Crossref
9. P. Bazarnik, A. Bartkowska, B. Romelczyk-Baishya, B. Adamczyk- Cieślak, J. Dai, Y. Huang, M. Lewandowska, T. G. Langdon. Jour. Alloys Comp. 846, 156380 (2020). Crossref
10. A. A. Nazarov, R. R. Mulyukov. Nanostructured Materials. In: Handbook of NanoScience, Engineering and Technology. (Ed. by W. A. Goddard III, D. Brenner, S. E. Lyshevski, G. J. Iafrate). CRC Press, Boca Raton (2002) pp. 22-1-22-41

11. L. Liu, Q. Deng, M. Su, M. An, R. Wang. Superlattices and Microstructures. 135, 106272 (2019). Crossref
12. G. J. Shi, J. G. Wang, Z. Y. Hou, Z. Wang, R. S. Liu. Modern Phys. Lett. B. 31 (27), 1750247 (2017). Crossref
13. B. Li, X. Zhai, Y. Cao, H. Zhao, Z. Wang, H. Liu, G. Fan. Forests. 9 (7), 397 (2018). Crossref
14. A. Behera, M. Ghosh. Mater. Today: Proc. 5 (9), 20647 (2018). Crossref
15. P. V. Polyakova, J. A. Baimova. IOP Conf. Ser.: Mater. Sci. Eng. 1008, 012052 (2021). Crossref
16. P. V. Polyakova, K. S. Nazarov, R. K. Khisamov, J. A. Baimova. Jour. Phys. Conf. Ser. 1435, 012065 (2020). Crossref
17. P. V. Polyakova, J. A. Pukhacheva, S. A. Shcherbinin, J. A. Baimova, R. R. Mulyukov. Appl. Sci. 11 (15), 6801 (2021). Crossref
18. E. V. Levchenko, A. V. Evteev, G. G. Löwisch, I. V. Belova, G. E. Murch. Intermetallics. 22, 193 (2012). Crossref
19. E. V. Levchenko, A. V. Evteev, T. Lorscheider, I. V. Belova, G. E. Murch. Comput. Mater. Sci. 79, 316 (2013). Crossref
20. G. M. Poletaev, I. V. Zorya, M. D. Starostenkov. Jour. Micromech. Molec. Phys. 03, 1850001 (2018). Crossref
21. M. A. Ghaffari, Y. Zhang, S. Xiao. Jour. Micromech. Molec. Phys. 02, 1750009 (2017). Crossref
22. I.V. Zorya, G. M. Poletaev, R. Rakitin, M.A. Ilyina, M. D. Starostenkov. Lett. Mater. 9 (2), 207 (2019). Crossref
23. P. V. Zakharov, G. Poletaev, M. D. Starostenkov, A. Cherednichenko. Lett. Mater. 7 (3), 296 (2017). (in Russian) [П. В. Захаров, Г. М. Полетаев, М. Д. Старостенков, А. И. Чередниченко. Письма о материалах. 7 (3), 296 (2017).] Crossref
24. R. I. Babicheva, S. V. Dmitriev, L. Bai, Y. Zhang, S. W. Kok, G. Kang, K. Zhou. Comput. Mater. Sci. 117, 445 (2016). Crossref
25. LAMMPS: https://www.lammps.org/ (accessed on 7 Dec. 2021)
26. OVITO: https://www.ovito.org/ (accessed on 7 Dec. 2021)
27. Common neighbor analysis (CNA): https://www.ovito.org/docs/current/reference/pipelines/modifiers/common_neighbor_analysis (accessed on 7 Dec. 2021)
28. R. R. Zope, Y. Mishin. Phys. Rev. B. 68 (2), 024102 (2003). Crossref
29. M. Kanani, A. Hartmaier, R. Janisch. Acta Mater. 106, 208 (2016). Crossref
30. D. Xu, H. Wang, R. Yang, P. Veyssiere. Acta Mater. 56 (5), 1065 (2008). Crossref
31. J. Chen, W. Chen, C. Wang. Appl. Phys. A. 126 (7), 493 (2020). Crossref
32. P. Li, L. Wang, B. Wang, S. Yan, M. Meng, X. Ji, K. Xue. Vacuum. 195, 110637 (2022). Crossref